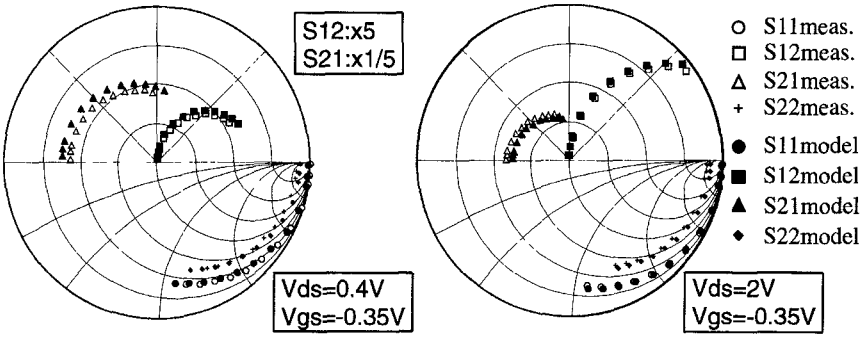

Fig. 5. Comparison of measured and modeled S-parameters. The left graph is typical characteristics in the linear region; the other is for the saturated region.

equivalent circuit, even for a certain bias condition in saturation region.

IV. Conclusion

A new nonlinear HEMT model is developed on the basis of the Curtice model for Harmonic Balance simulation. Terms for leakage current for subthreshold voltage, drain voltage dependence for knee voltage, drain conductance and threshold voltage, the transconductance enhancement by DX centers, and the bias dependence of capacitance are introduced. By adopting this model for a pseudomorphic double-recessed gate HEMT, average errors of 2.6% for dc current and 10% S-parameters are obtained.

References

[1] L. F. Lester, P. M. Smith, P. Ho, P. C. Chao, R. C. Tiberio, K. H. G. Duh, and E. D. Wolf, "0.15 μm gate length double recess pseudomorphic HEMT with F_{max} of 350 GHz," in *IEDM'88*, 1988, pp. 172–175.

[2] H. Daembkes, Ed., *Modulation-Doped Field-Effect Transistors: Applications and Circuits*. New York: IEEE Press, 1991.

[3] A. H. Ng, R. Khoie, and R. Venkat, "A two-dimensional self-consistent numerical model for high electron mobility transistor," *IEEE Trans. Electron Devices*, vol. 38, p. 852, 1991.

[4] W. R. Curtice and M. Ettenberg; "A nonlinear GaAs FET model for use in the design of output circuits for power amplifiers," *IEEE Trans. Microwave Theory Tech.*, vol. MTT-33, 1985.

[5] H. Rohdin and P. Roblin; "A MODFET DC model with improved pinchoff and saturation characteristics," *IEEE Trans. Electron Devices*, vol. ED-33, p. 664, 1986.

[6] T. Tanimoto, M. Kudo, T. Mishima, M. Mori, and M. Yamane, "Double recessed gate InGaAs pseudomorphic channel HEMT's for low current operation," ICICE Tech. Rep., vol. ED91-149, pp. 79–86, 1992 (in Japanese).

[7] H. Mizuta, K. Yamaguchi, M. Yamane, T. Tanoue, and S. Takahashi, "Two-dimensional numerical simulation of Fermi-level pinning phenomena due to DX centers in AlGaAs/GaAs HEMT's," *IEEE Trans. Electron Devices*, vol. 36, pp. 2307–2314, 1989.

Quasi-TEM Analysis of Coplanar Waveguides with an Inhomogeneous Semiconductor Substrate

Jean-Fu Kiang

Abstract— **In this paper, we study the normalized wavelength and attenuation constant of coplanar waveguides with a finite metal thickness. The substrate is a lossy inhomogeneous insulator–semiconductor, and the conductor is assumed perfect. Electroquasi-static approximation is used to derive a Laplace's equation with a complex permittivity in each inhomogeneous layer, from which the eigenmodes are obtained. Proper boundary conditions between contiguous layers are applied to calculate the charge distribution on the center conductor. The effects of the insulator depth and semiconductor conductivity on the normalized wavelength and attenuation constant are analyzed.**

I. Introduction

The doping profile in the semiconductor substrate affects the propagation characteristics of microstrip lines and coplanar waveguides significantly. In [1] and [2], the propagation characteristics of coplanar waveguides fabricated on an insulator–semiconductor substrate have been studied. For Schottky-contact microstrip lines, the bias voltage applied to the metal line creates a localized depletion zone around the metallization [3]. Due to the conductive loss in the semiconductor, slow wave modes with attenuation are observed [3]–[8]. The slow wave factor and the attenuation constant of either microstrip lines or coplanar waveguides have been studied using parallel plate waveguide model [3], full-wave finite element method [6], finite-difference time-domain method [7], and method of lines [8].

As long as the cross-section dimension of the coplanar waveguide is a small fraction of one wavelength, the quasi-TEM analysis can be applied to model its propagation properties even up to the millimeter wave range. In [9], an electrostatic formulation is used to calculate the capacitance and inductance matrices on which the quasi-TEM analysis is based. Resistive loss due to imperfect conduct has been studied by using quasi-TEM approach [10] and conformal mapping technique [11]. In [12], both the semiconductor loss and conductor loss are considered. Overall, the inhomogeneities of substrate is only analyzed in [8].

Manuscript received November 10, 1995; revised May 24, 1996. This work was supported by the National Science Council, Taiwan, ROC under Contract NSC 85-2213-E005-010.

The author is with Department of Electrical Engineering, National Chung-Hsing University, Taichung, Taiwan, ROC.

Publisher Item Identifier S 0018-9480(96)06389-2.

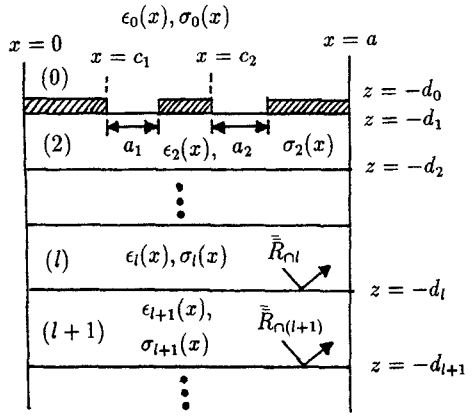

Fig. 1. Geometrical configuration of a coplanar waveguide with a finite strip thickness in a lossy inhomogeneous stratified medium.

In this paper, we propose a new approach to solve the potential distribution of coplanar waveguides on an inhomogeneous and lossy substrate. The potential in each inhomogeneous layer can be expressed in terms of only a few eigenmodes which are obtained by solving the Laplace's equation with a complex permittivity. Reflection matrices are also defined to further reduce the number of unknowns. In contrast, the finite difference and finite element type of approaches require many unknowns to describe the potential distribution. The complex charge distribution on the center conductor is then calculated and used in the subsequent quasi-TEM analysis to study the normalized wavelength and attenuation constant.

II. Formulation

Assuming that the dimension of interest is much smaller than one wavelength, hence the electric field can be expressed as the gradient of a potential $\bar{E} = -\nabla\phi$. From the charge conservation and the Ohm's law, we have $\nabla \cdot \sigma\bar{E} = i\omega\rho$. Combining these two equations with the Gauss' law, a Laplace's equation with a complex permittivity is obtained

$$\nabla \cdot \tilde{\epsilon}\nabla\phi = 0 \tag{1}$$

where $\tilde{\epsilon} = \epsilon + i\sigma/\omega$.

In Fig. 1, we show the configuration of a coplanar waveguide in a lossy inhomogeneous stratified medium. The permittivity and conductivity in each layer is a piecewise continuous function of x and is independent of z. Two perfect electric conductor walls are located at $x = 0$ and $x = a$ as the potential reference.

Explicitly, the Laplace's equation in layer (m) is

$$\left(\tilde{\epsilon}_m^{-1}(x)\frac{\partial}{\partial x}\tilde{\epsilon}_m(x)\frac{\partial}{\partial x} + \frac{\partial^2}{\partial z^2}\right)\phi(x,z) = 0. \tag{2}$$

By the separation of variables, $\phi(x,z)$ can be expressed as a product $\psi(x)\eta(z)$ where

$$\begin{aligned}\tilde{\epsilon}_m^{-1}(x)\frac{d}{dx}\tilde{\epsilon}_m(x)\frac{d}{dx}\psi(x) &= -k^2\psi(x)\\ \frac{d^2}{dz^2}\eta(z) &= k^2\eta(z).\end{aligned} \tag{3}$$

Next, choose a set of basis functions $S_p(x) = \sqrt{2/a}\sin(\alpha_p x)$ with $\alpha_p = p\pi/a$ to represent $\psi(x)$. These basis functions satisfy the orthonormality specification that $\langle S_q(x), S_p(x)\rangle = \delta_{qp}$ with the inner product defined over the interval $[0, a]$. The nth eigensolution $\psi_n(x)$ can thus be expanded by these basis functions as $\psi_n(x) = \sum_{p=1}^{N} b_{np}S_p(x)$. Then, substitute the expansion into (3), take the inner product of $S_q(x)$ with the resulting equation, and apply the orthonormality property of $S_p(x)$'s to obtain a matrix equation from which to solve for the eigenvalues k_n^2 and their associated eigenvectors.

The potential in layer (l) with $l > 1$ can be expressed in terms of the eigenfunctions as

$$\phi_l(x,z) = \bar{\psi}_l^t(x) \cdot \left[e^{-\bar{\bar{K}}_l z_l} \cdot \bar{\bar{R}}_{\cap l} + e^{\bar{\bar{K}}_l z_l}\right] \cdot \bar{B}_l \tag{4}$$

where $z_l = z + d_l$, $\bar{\bar{K}}_l = \text{diag.}[k_1, \ldots, k_N]$, $e^{\pm\bar{\bar{K}}_l z_l} = \text{diag.}[e^{\pm k_1 z_l}, \ldots, e^{\pm k_N z_l}]$, and $\bar{\psi}_l^t(x) = [\psi_1(x), \ldots, \psi_N(x)]$ are eigensolutions in layer (l). By matching the boundary condition that the potential and the normal electric flux density are continuous at $z = -d_l$, a recursive relation between the reflection matrices $\bar{\bar{R}}_{\cap l}$'s can be obtained.

The potential in layer (0) can be expressed as

$$\phi_0(x,z) = \bar{\psi}_0^t(x) \cdot e^{-\bar{\bar{K}}_0 z_0} \cdot \bar{A}_0. \tag{5}$$

The potential in the two gaps ($c_1 \le x \le c_1 + a_1$ and $c_2 \le x \le c_2 + a_2$) of layer (1) can be expressed as

$$\begin{aligned}&\phi_1(x,z)\\ &= \begin{cases}\phi_{1a}(x,z) = Vx_1/a_1\\ \qquad +\sum_{n=1}^{N_1}\sin(\alpha_{1n}x_1)[u_{1n}e^{-\alpha_{1n}z_1} + v_{1n}e^{\alpha_{1n}z_1}],\\ \qquad c_1 \le x \le c_1 + a_1\\ \phi_{1b}(x,z) = V(1 - x_2/a_2)\\ \qquad +\sum_{n=1}^{N_2}\sin(\alpha_{2n}x_2)[u_{2n}e^{-\alpha_{2n}z_1} + v_{2n}e^{\alpha_{2n}z_1}],\\ \qquad c_2 \le x \le c_2 + a_2\end{cases}\end{aligned} \tag{6}$$

where $x_i = x - c_i$ and $\alpha_{in} = n\pi/a_i$ with $i = 1, 2$. Impose the boundary condition that the potential is continuous at $z = -d_0$ ($z = -d_1$), then take the inner product of $\tilde{\epsilon}_0(x)\bar{\psi}_0(x)$ ($\tilde{\epsilon}_2(x)\bar{\psi}_2(x)$) with the resulting equation to obtain (A) [(B)]. Next, impose the boundary condition that the normal electric flux density is continuous at $z = -d_0$ ($z = -d_1$) over the gaps between the conductors, then take the inner product of $\sin(\bar{\alpha}_i x_i)$ with the resulting equation to obtain (C) [(D)].

The total complex charge per unit length around the center strip, Q, can be calculated by solving (A), (B), (C), and (D). Then, define the complex capacitance per unit length as $C = Q/V$, and calculate the propagation constant of the quasi-TEM mode as $k_y = \beta + i\alpha = \omega\sqrt{\mu_0\epsilon_0}\sqrt{C/C_0}$ where C_0 is the capacitance per unit length with the whole stratified medium replaced by free space.

III. Numerical Results

In Fig. 2, we show the normalized wavelength and the attenuation constant of a coplanar waveguide on an insulator–semiconductor–insulator substrate. Since the dielectric constant of the semiconductor is higher than that of the top insulator layer, the effective dielectric constant of the dominant mode decreases and the normalized wavelength increases as the semiconductor layer gets thinner. As the semiconductor layer gets thinner, the electric fields pass through less semiconductor area, hence the attenuation constant decreases. When $t_1/(t_1 + t_2)$ is above 0.8, the bottom insulator with high dielectric constant makes the field distribution shift downward, and the field in the semiconductor layer becomes stronger. Thus the attenuation constant increases slightly. The deviation between our results and the reference data

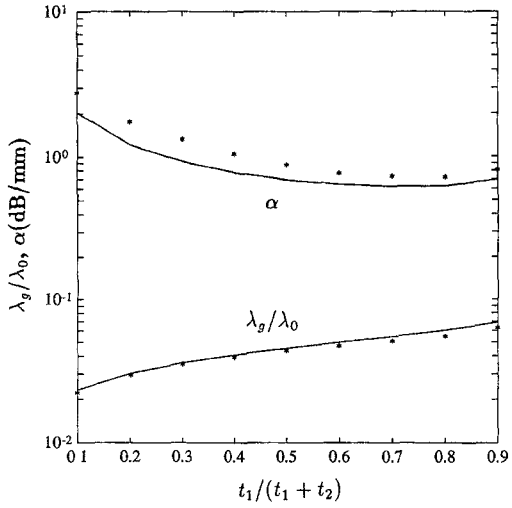

(a)

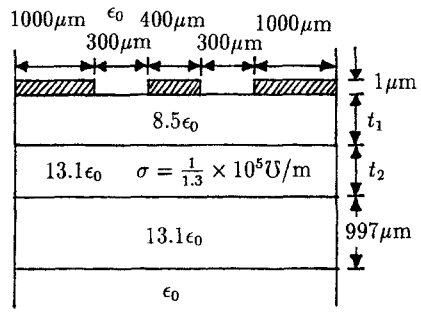

(b)

Fig. 2. Normalized wavelength and attenuation constant of a coplanar waveguide on an insulator–semiconductor–insulator substrate (results from [2]).

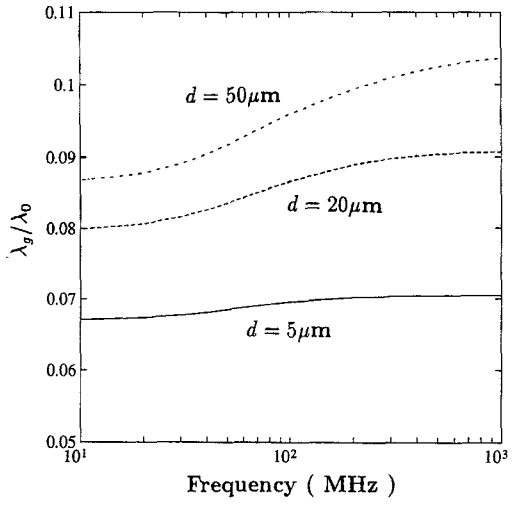

(a)

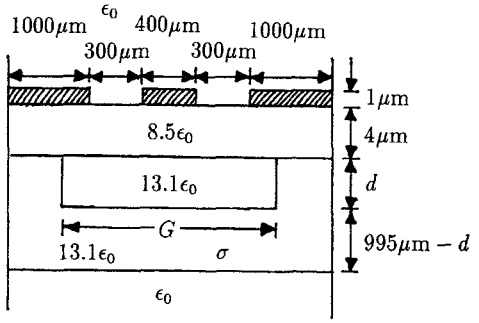

(b)

Fig. 3. Normalized wavelength of a coplanar waveguide on an insulator–semiconductor substrate with the insulator depth as parameter, $G = 400$ μm, $\sigma = 10^5$ U/m.

from [2] is reasonably small considering that the full-wave approach is used in [2].

In Fig. 3, we show the normalized wavelength of a coplanar waveguide on an inhomogeneous insulator–semiconductor substrate. Since the semiconductor attenuates the dominant mode, an insulator region may be fabricated into the semiconductor substrate to reduce the loss. Less loss is incurred as the insulator depth increases, hence the phase velocity increases. However, the attenuation constant in Fig. 4 shows that the structure with a deeper insulator region has a higher attenuation constant, which is opposite to what we have expected.

So, we calculate the propagation constant with the same geometrical and electrical parameters except that the conductivity in the semiconductor is set to 0.1 U/m. The normalized wavelength shows little deviation among three different insulator depths because the loss is smaller than in the case with $\sigma = 10^5$ U/m. The attenuation constants are consistent with what we have expected that deeper insulator gives less loss. We also observe that the attenuation constant reaches a maximum then decreases as the frequency increases. It is because the field distribution concentrates more around the center conductor at high frequencies.

To understand the variation of phase velocity and attenuation constant with frequency, we analyze the same structure with different semiconductor conductivities. The results are shown in Figs. 5 and 6. The phase velocity stays in a *low plains* at low frequencies, and transits to a *high plateau* at high frequencies. The transition occurs at lower frequency when the conductivity is smaller. At low frequencies,

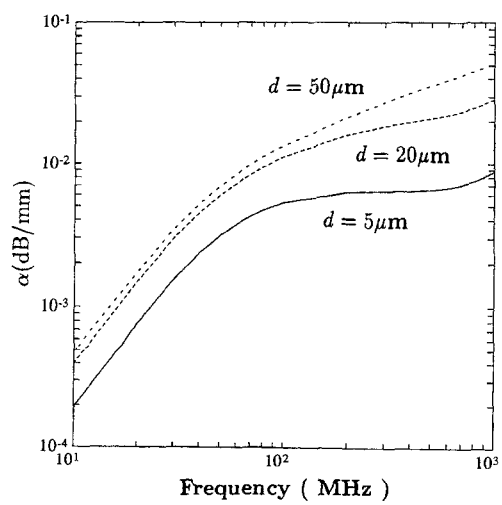

Fig. 4. Attenuation constant of a coplanar waveguide on an insulator–semiconductor substrate with the insulator depth as parameter, $G = 400$ μm, $\sigma = 10^5$ U/m, the other parameters are the same as in Fig. 3.

the attenuation constant with a low conductivity is larger than that with a high conductivity. As the phase velocity transits from the low plains to the high plateau, the attenuation increases. When the phase

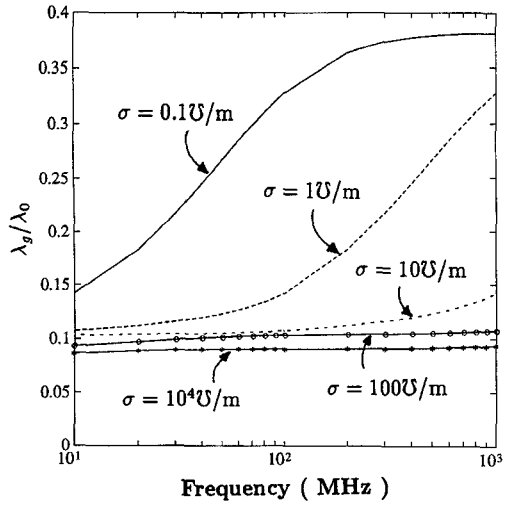

Fig. 5. Normalized wavelength of a coplanar waveguide on an insulator–semiconductor substrate with the semiconductor conductivity as parameter, $G = 400\ \mu m$, $d = 20\ \mu m$, the other parameters are the same as in Fig. 3.

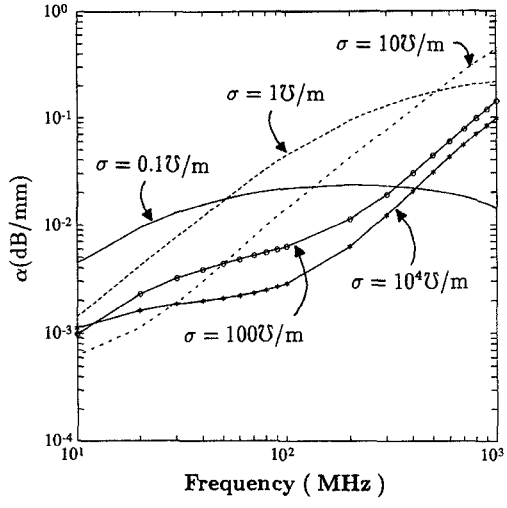

Fig. 6. Attenuation constant of a coplanar waveguide on an insulator–semiconductor substrate with the semiconductor conductivity as parameter, $G = 400\ \mu m$, $d = 20\ \mu m$, the other parameters are the same as in Fig. 3.

velocity falls in the high plateau, the fields tend to concentrate around the center conductor, and the attenuation constant decreases. With a higher conductivity, the rise of the attenuation constant occurs at a higher frequency, and the magnitude is larger than that with a low conductivity.

IV. Conclusion

The variations of normalized wavelength and attenuation constant with frequency of a coplanar waveguide on an inhomogeneous insulator semiconductor substrate have been analyzed. A new eigenmode approach is first proposed to solve the Laplace's equation with a complex permittivity to obtain the potential distribution in an inhomogeneous stratified medium. The charge distribution on the center conductor is then used in the quasi-TEM analysis to obtain the propagation constant with different semiconductor conductivities and insulator depths. A frequency range exists where the phase velocity rises from a low plains to a high plateau, and the attenuation constant rises to a maximum then decreases. The transit frequency is higher with a higher semiconductor conductivity.

Acknowledgment

The author would like to thank the reviewers for their useful comments.

References

[1] Y. Fukuoka, Y.-C. Shih, and T. Itoh, "Analysis of slow-wave coplanar waveguide for monolithic integrated circuits," *IEEE Trans. Microwave Theory Tech.*, vol. MTT-31, pp. 567–573, July 1983.

[2] R. Sorrentino, G. Leuzzi, and A. Silbermann, "Characteristics of metal-insulator-semiconductor coplanar waveguides for monolithic microwave circuits," *IEEE Trans. Microwave Theory Tech.*, vol. MTT-32, pp. 410–416, Apr. 1984.

[3] D. Jager, "Slow-wave propagation along variable Schottky-contact microstrip line," *IEEE Trans. Microwave Theory Tech.*, vol. MTT-24, pp. 566–573, Sept. 1976.

[4] H. Hasegawa, M. Furukawa, and H. Yanai, "Properties of microstrip line on Si-SiO_2 system," *IEEE Trans. Microwave Theory Tech.*, vol. MTT-19, pp. 869–881, Nov. 1971.

[5] P. Pribetich, C. Seguinot, and P. Kennis, "Systematic determination of the propagation characteristics of coplanar lines on semiconductor substrate," *IEEE Trans. Microwave Theory Tech.*, vol. 39, pp. 1083–1089, July 1991.

[6] J.-F. Lee, "Finite element analysis of lossy dielectric waveguides," *IEEE Trans. Microwave Theory Tech.*, vol. 42, pp. 1025–1031, June 1994.

[7] T. Shibata and E. Sano, "Characterization of MIS structure coplanar transmission lines for investigation of signal propagation in integrated circuits," *IEEE Trans. Microwave Theory Tech.*, vol. 38, pp. 881–890, July 1990.

[8] K. Wu and R. Vahldieck, "Hybrid-mode analysis of homogeneously and inhomogeneously doped low-loss slow-wave coplanar transmission lines," *IEEE Trans. Microwave Theory Tech.*, vol. 39, pp. 1348–1360, Aug. 1991.

[9] E. Drake, F. Medina, and M. Horno, "Quick computation of $[C]$ and $[L]$ matrices of generalized multiconductor coplanar waveguide transmission lines," *IEEE Trans. Microwave Theory Tech.*, vol. 42, pp. 2328–2335, Dec. 1994.

[10] H. Klingbeil and W. Heinrich, "Calculation of CPW A.C. resistance and inductance using a quasi-static mode-matching approach," *IEEE Trans. Microwave Theory Tech.*, vol. 42, pp. 1004–1007, June 1994.

[11] G. Ghione, "A CAD-oriented analytical model for the losses of general asymmetric coplanar lines in hybrid and monolithic MIC's," *IEEE Trans. Microwave Theory Tech.*, vol. 41, pp. 1499–1510, Sept. 1993.

[12] Y. R. Kwon, V. M. Hietala, and K. S. Champlin, "Quasi-TEM analysis of "slow-wave" mode propagation on coplanar microstructure MIS transmission lines," *IEEE Trans. Microwave Theory Tech.*, vol. MTT-35, pp. 545–551, June 1987.